Destabilizing Mutations Alter the Hydrogen Exchange Mechanism in Ribonuclease A

Marta Bruix,* Marc Ribó,† Antoni Benito,† Douglas V. Laurents,* Manuel Rico,* and Maria Vilanova†
*Instituto de Química Física "Rocasolano", Consejo Superior de Investigaciones Científicas, 28006 Madrid, Spain; and †Laboratori d'Enginyeria de Proteïnes, Departament de Biologia, Facultat de Ciències, Universitat de Girona, Campus Montilivi, 17071 Girona, Spain

ABSTRACT The effect of strongly destabilizing mutations, I106A and V108G of Ribonuclease A (RNase A), on its structure and stability has been determined by NMR. The solution structures of these variants are essentially equivalent to RNase A. The exchange rates of the most protected amide protons in RNase A (35°C), the I106A variant (35°C), and the V108G variant (10°C) yield stability values of 9.9, 6.0, and 6.8 kcal/mol, respectively, when analyzed assuming an EX2 exchange mechanism. Thus, the destabilization induced by these mutations is propagated throughout the protein. Simulation of RNase A hydrogen exchange indicates that the most protected protons in RNase A and the V108G variant exchange via the EX2 regime, whereas those of I106A exchange through a mixed EX1 + EX2 process. It is striking that a single point mutation can alter the overall exchange mechanism. Thus, destabilizing mutations joins high temperatures, high pH and the presence of denaturating agents as a factor that induces EX1 exchange in proteins. The calculations also indicate a shift from the EX2 to the EX1 mechanism for less protected groups within the same protein. This should be borne in mind when interpreting exchange data as a measure of local stability in less protected regions.

INTRODUCTION

The ability of enzymes to carry out molecular jobs with high efficacy and specificity make them good candidates for a variety of applications including medicine, biotechnology, or nanotechnology. Most of these applications require protein modifications to improve some fundamental characteristics, like stability, with respect to the wild-type protein. Ribonuclease A (RNase A) (Fig. 1) is one of the most and best studied enzymes from the structural, enzymatic, folding and stability perspectives (1,2). Recently some designed variants and natural homologs of RNase A have found important applications in biomedicine. On the other hand, point mutations strongly destabilizing the native structure of proteins can lead to loss of function or to the formation of non-native and toxic amyloid conformations, which have been implicated in over 20 mortal human diseases (3). In RNase A, residues I106 and V108 are buried deep in the hydrophobic core and are thought to contribute to the early folding of the protein. The contribution of these residues to the stability and folding of RNase A has been probed by mutagenesis combined with calorimetry, pressure or heat induced denaturation and their substitution was found to dramatically destabilize the folded state. The substitutions of I106A, V108A, and V108G destabilized RNase A by 4.9, 4.8, and 9.3 kcal/mol, respectively (4–7). The main objective is to determine how these destabilizing substitutions affect the structure and stability of RNase A at individual amide groups.

In recent years, hydrogen/deuterium (H/D) exchange experiments followed by NMR has become the major biophysical tool to obtain the conformational stability values at the residue level (8,9). This method has been applied to understand factors behind the protein stability of several systems including RNase A, RNase S, cytochrome c, cytochrome b_{562}, RNase H, ovomucoid third domain, RNase T1, RNase Sa, barnase, BPTI, barstar, SH3 domain, hen lysozyme, T4 lysozyme, staphylococcal nuclease, and others (see (10) and references therein). However, the local stability can be measured only when the unfolding and refolding kinetics of a given amide group are fast compared to the intrinsic exchange rate in the EX2 exchange limit (see below), representing the exchange reaction of a protected amide as

$$\text{closed}\,(H) \underset{k_{cl}}{\overset{k_{op}}{\Leftrightarrow}} \text{open}\,(H) \overset{k_{rc}}{\Rightarrow} \text{open}\,(D) \underset{k_{op}}{\overset{k_{cl}}{\Leftrightarrow}} \text{closed}\,(D), \quad (1)$$

where k_{op} and k_{cl} are the rate constants for the opening or unfolding and closing or folding events respectively, and k_{rc} is the intrinsic exchange rate for the competent amide group.

The observed rate constant for the overall process shown in Eq. 1 in strongly native conditions, i.e., $k_{cl} \gg k_{op}$, is (11)

$$k_{ex} = k_{op}k_{rc}/(k_{op} + k_{cl} + k_{rc}). \quad (2)$$

There are two limiting mechanisms for exchange (11). In the EX1 limit $k_{cl} \ll k_{rc}$ and each opening fluctuation leads to exchange and Eq. 2 simplifies to

$$k_{ex} = k_{op} \quad (3)$$

In the other limit, where $k_{cl} \gg k_{rc}$ (EX2 limit), the chemical exchange is the rate-limiting step and Eq. 2 reduces to

$$k_{ex} = (k_{op}/k_{cl})k_{rc} = K_{op}k_{rc}, \quad (4)$$

where K_{op} is defined as the equilibrium constant or the conformational transition between the open and closed states.

Submitted September 30, 2007, and accepted for publication November 16, 2007.

Address reprint requests to M. Bruix, E-mail: mbruix@iqfr.csic.es.

Editor: Arthur G. Palmer 3rd.

© 2008 by the Biophysical Society

0006-3495/08/03/2297/09 $2.00

doi: 10.1529/biophysj.107.122952

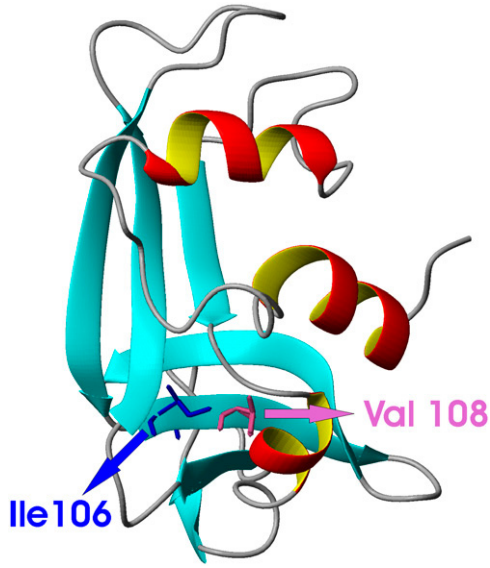

FIGURE 1 Ribbon representation of the 3D structure of RNase A based on the solution structure determined by Santoro et al. (31) and generated using MolMol (50). Side chains of Ile^{106} (*blue*) and Val^{108} (*pink*) are represented.

Therefore, whether a system exchanges by the EX1, EX2, or a mixture of EX1 + EX2, depends on the relation of the different unfolding, refolding, and intrinsic exchange rates. It is known that stabilizing conditions, lower temperature, and the absence of denaturating agents favor the EX2 process as they increase k_{cl}. Moreover, lower pH values favor the EXII regime by decreasing k_{rc}. Most exchange studies to date have been carried out under the EX2 regime. On the other hand, increasing the intrinsic rate of exchange (k_{rc}) or decreasing the refolding rate (k_{cl}) can shift the mechanism to EX1. Exchange via the EX1 regime has been used to measure the unfolding rates of individual amide groups (12). Three factors promoting the shift toward EX1 exchange conditions have been identified in several proteins including RNase A. These factors include: 1), raising the pH; 2), adding denaturants like urea or GdmCl; and 3), heating the sample (13). One may expect that destabilizing mutations, which lower k_{cl}, could also shift the exchange mechanism from EX2 to EXI, but to date no systematic study including strongly destabilized variants has been done. In general, mutants with similar stability to wild-type have been used to identify protons that exchange through global unfolding by comparing exchange in wild-type and mutant proteins (14). This type of approach has been done for RNase A and RNase S, a subtilisin-cleaved form (15,16). To carry out this analysis, it is necessary that the mutation does not severely alter the tertiary structure.

We have studied used NMR to measure how highly destabilizing mutations at key core positions, Ile^{106} and Val^{108}, affect the structure and H/D exchange of RNase A. Using values for k_{op}, k_{cl}, and k_{rc}, the exchange process was simulated to identify the EX1 and EX2 exchange regime boundaries as a function of stability. Two different situations can be predicted. First, the mutation destabilizes the region and changes locally the exchange process; second, the single mutation changes the mechanism of exchange globally.

MATERIALS AND METHODS

Protein samples

Wild-type and I106A and V108G RNase A mutants (recombinant forms) were expressed in *Escherichia coli* and purified as published (4,17). RNase A and its variants were uniformly labeled with ^{15}N as described previously (18) using labeled Martek9 medium from Spectra Stable Isotopes (Spectra Gases, Columbia, MD). Double-distilled water was deionized using a MilliQ (Millipore, Bedford, MA) system. All other reagents were of the highest purity grade available.

NMR spectroscopy

Unlabeled and labeled NMR samples containing ~1 mM RNase A, wild-type (wt), or variants, were dissolved in 0.5 ml 90% H_2O/10% D_2O or D_2O (>99.9% atom D) (Apollo Science, Derbyshire, UK). All samples contained 0.2 M NaCl and the pH* (pH not corrected for isotope effects) was adjusted to 5.4. Sodium 4,4 dimethyl-4-silapentane-1-sulfonate was used as the internal chemical shift standard. All NMR experiments were carried out using a Bruker AMX-600 spectrometer equipped with a triple resonance probe and a z axis pulse field gradient. NMR assignments for RNase A wt and I106A mutant were obtained at 35°C and those of V108G variant at 10°C. NMR data were processed on a Silicon Graphics workstation using XWinNMR package and analyzed using version 3.3 of the program ANSIG (19). The spectra of the mutant variants were assigned at pH 5.4, following the standard NOE-based methodology as well as the reported assignment of the wild-type protein (20,21). 2D ^1H-^1H TOCSY (22) and NOESY (23) and 3D ^{15}N-^1H HSQC-TOCSY and ^{15}N-^1H HSQC-NOESY (24) spectra with mixing times of 60 and 50 ms, respectively, were recorded by using standard pulse sequences.

Hydrogen exchange by NMR spectroscopy

The exchange of amide protons with solvent deuterons was started by dissolving lyophilized, protonated wild-type ^{15}N-RNase A, ^{15}N-I106A, or ^{15}N-V108G variants into deuterated solvent. The temperature and pH* of the exchange experiments were the same as those used in the assignment process (see above). The pH* 5.4 was chosen because it is high enough that the exchange will be fast enough to allow the measurement of the exchange of the slowest exchanging groups, but low enough so that exchange will proceed by the EX2 mechanism for wild-type RNase A (15). The hydrogen exchange rates were determined by integrating the volume of ^1H-^{15}N amide crosspeaks in a series of HSQC spectra (25). After a dead time (≈30 min), a series of HSQC spectra were recorded consecutively. Spectra were processed with the XwinNMR package, and correlation crosspeaks were integrated with a macro within the UXNMR program. A single exponential decay function was fit to the data to determine the observed exchange rate, k_{ex}. The obtained k_{ex} values are reported in a Supplementary Table. The intrinsic exchange rates for fully denatured proteins, k_{rc}, were calculated using the parameters reported by Englander et al. (26) corrected for pH* 5.4 and temperature. Using equations described therein (26), the protection factors, i.e., the ratio of the intrinsic and observed exchange rates of the individual groups, were determined. When exchange is governed by the EX2 regime, the conformational stability, ΔG_{HX}, of each amide group can be calculated from the protection factor

$$\Delta G_{HX} = -RT\ln(k_{ex}/k_{rc}) = -RT\ln K_{op} = -RT\ln(1/P), \quad (5)$$

where K_{op} is the local or global equilibrium constant for the opening reaction and P the protection factor.

Uncertainty analysis

The uncertainties in the exchange rates varied from ±5% in favorable cases, to ±15% for less favorable cases. The latter occurs when amide protons exchanged relatively fast or slow relative to the acquisition of NMR spectra. Due to the logarithmic dependence of the conformational free energies on the exchange rates, these uncertainties propagate to relatively small values in the free energies; in favorable cases, the uncertainty range (1σ) of ΔG_{HX} is ~±1%.

Simulation of hydrogen exchange mechanism of RNase A

As described in the Introduction, the exchange process can be modeled as a two-step reaction for each amide hydrogen wherein a closed conformation first opens and then permits exchange with a rate constant, k_{rc}, that depends on temperature, pH, and the neighboring side chains (11,26,27). We have determined recently the dependence of the global unfolding (k_{op}) and refolding (k_{cl}) rates of RNase A at different temperatures for a fluorescent variant of RNase A (Y115W) whose stability is similar to that of the wild-type protein (4) using pressure induced denaturation (28). At 35°C and pH 5.0 and extrapolating to 1 atm pressure, k_{cl} and k_{op} of RNase A Y115W are 25.5 s^{-1} and 1.12×10^{-5} s^{-1}, respectively. First, a range of nominal stability values, ΔG_{nom} (0–10 kcal/mol) was chosen. As the ΔG_{nom} decreases, k_{cl} will decrease and k_{op} will increase. The values of k_{cl} and k_{op} at different ΔG_{nom} values was calculated using

$$\Delta k_{(\text{cl or op})} = e^{-\Delta\Delta G\text{nom}\times f/RT}, \quad (6)$$

where R is the gas constant, T is the absolute temperature, and f is defined as the fraction of the change in ΔG_{nom} that affects k_{cl} or k_{op}. This value f was calculated from the slopes of the refolding and unfolding limbs, m_f and m_u, respectively, of the chevron plot (ln k versus pressure) of RNase A Y115W at 35°C and pH 5.0, and is

$$f = m_f/(m_f + m_u)\ (\text{for } \Delta k_{cl}) \quad (7a)$$

$$f = m_u/(m_f + m_u)\ (\text{for } \Delta k_{op}). \quad (7b)$$

The value of f was found to be ~0.5. Values for k_{cl} and k_{op} at pH 5.4 and 10°C were calculated from the temperature dependence of the pressure-induced unfolding and refolding rates of Y115W RNase A (28), and are similar to those obtained previously by another group for the GdmCl-induced unfolding and refolding of wild-type RNase A at pH 6.0 10°C (29). Using these rates and the intrinsic exchange rate (k_{rc}) at these conditions, pH 5.4*, 35°C and pH 5.4*, 10°C, we have simulated the exchange using the program KINSIM (30) and determined the overall exchange rates ($k_{ex\ sim}$) at different stability values. Additionally, on the bases of these $k_{ex\ sim}$ and k_{rc} values at a given temperature, the theoretical $\Delta G_{HX\ sim}$ values were calculated applying Eq. (5).

RESULTS

NMR chemical shift analysis

Assignment of the ^1H and ^{15}N chemical shifts of the variants was carried out to determine if the three-dimensional structure (3D) of the wild-type enzyme (31) is preserved in solution. A comparison of the backbone NH and Hα chemical shift deviations for V108G variant (the least stable mutant) with respect to the chemical shifts of wild-type (32) protein is shown in Fig. 2. Overall, chemical shift differences ($\Delta\delta = \delta_{wt} - \delta_{mut}$) are small. Profiles corresponding to HN and Hα protons show that most of the chemical shifts are within 0.1 and 0.05 ppm, respectively, of their values in wild-type

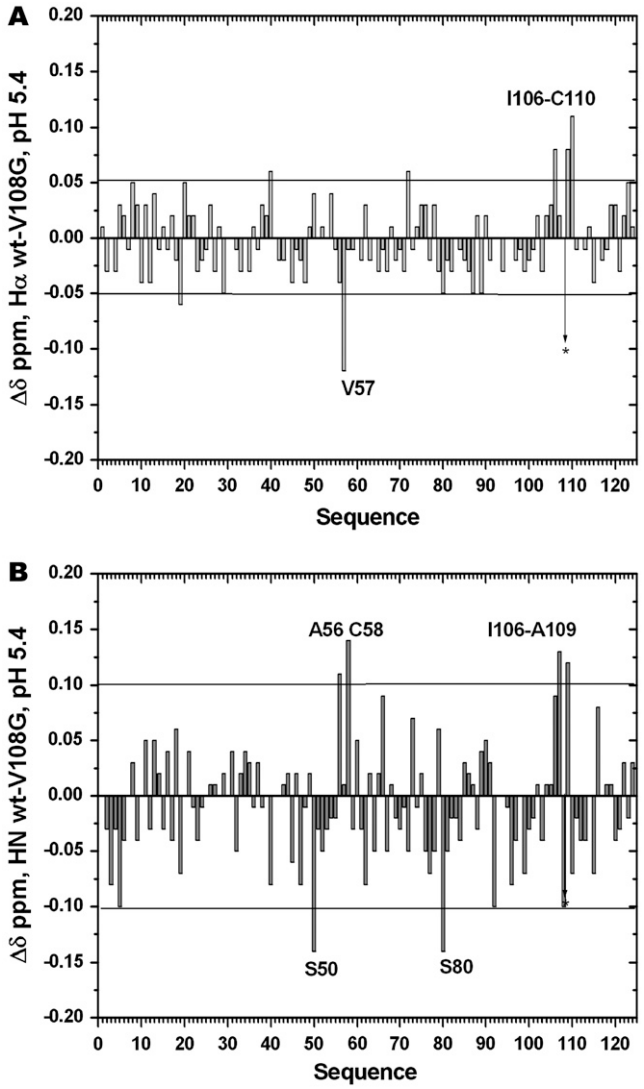

FIGURE 2 Plots of the chemical shift differences between wt RNase A and V108 variant at pH* 5.4 and 10°C. (*A*) Hα protons. (*B*) HN protons. Arrows and stars indicate the point mutation.

RNase A. These changes show that the main differences are localized near the mutation, although some differences in the Ala^{56}-Cys^{58} segment are observed, which could be attributed to small structural rearrangements due to the loss of interactions between the methyl groups of Val^{108} and Val^{57} in the wt RNase A that are absent in the variant V108G. Regarding the ^{1}HN signals of Ser^{50} and Ser^{80}, these nuclei are exquisitely sensitive to pH and temperature differences and shift 1.0 ppm and 1.9 ppm, respectively, on raising the pH from 2 to 8. Therefore, the changes observed for these protons in the V108G variant are not likely due to the mutation but can be attributed to slight differences in the measured pH or temperature.

Qualitative information about possible changes in the side chain conformations can be also evaluated on the basis of perturbed ^{1}H chemical shift. In general, changes are also

small, on the same order of that of the backbone atoms. Thus, all the NMR data point toward the conclusion that the 3D solution structures of these mutants are essentially the same as that of wt RNase A, apart from small conformational changes near the mutated site.

Residue-level and global stability of ^{15}N-RNase A wild-type from H/D exchange measurements

Previous hydrogen exchange studies monitored by NMR under different solution conditions were carried out with nonlabeled and commercial RNase A: pH 5.5 and 34°C (33); pH 6.5, pH 7.4, and 35°C (34); and pH 5.4, pH 6.0, and 15°C, 25°C, 35°C (15). In this study, we have carried out a similar study with recombinant ^{15}N-labeled RNase A at pH 5.4 and 35°C. These experimental conditions were chosen to facilitate the comparison with the results mentioned previously based on homonuclear NMR experiments. Because ^{1}H-^{15}N-HSQC experiments can be recorded quickly, more spectra can be recorded and with reduced dead times, thereby increasing the number of NHs that can be monitored and the precision of the measurements. The corresponding protection factors and conformational free energies are shown in Fig. 3. Amide protons with rate constants $>\approx 1.3\ hr^{-1}$ exchanged in the dead time of the NMR spectral acquisition and thus define the lower limit for protection factors of 500 to 1000, depending on the side chains adjacent to the amide group. Under our experimental conditions, all the residues exchange during the total experimental time of ~21 days. As can be seen, the exchange rates and corresponding protection factors of neighboring amide protons vary widely, which is inline with EX2 governed exchange (see below). The global ΔG_{HX} measured by NMR is ~10 kcal/mol for recombinant RNase A at pH 5.4 and 35°C. The most protected amide protons are located in secondary elements: the C-termini of α-helices, internal regions of the β-strands, and residues Arg^{10}, Glu^{11}, His^{12}, and Met^{13} that anchor the N-terminal α-helix to the protein core. The slowest amide protons belong to Met^{13} in α-helix I, Gln^{55}, and Cys^{58} in α-helix III and Ala^{109} in β-strand V. Their corresponding individual ΔG_{HX} values are 9.9, 9.6, 9.9, and 10.0 kcal/mol respectively.

Simulation of the H-exchange kinetics and stability of RNase A

Fig. 4 *A* shows the simulated H-exchange mechanism of RNase A as a function of protein stability at 35°C and pH* 5.4. Above 6 kcal/mol, $k_{cl} \gg k_{rc}$ so in these conditions RNase A exchange will proceed by the EX2 mechanism as was found previously (15,34–36). On the contrary, below 2 kcal/mol, the $k_{rc} \gg k_{cl}$ and the exchange regime changes to the EX1 mechanism and is governed by the opening rate, k_{op}. For protein stabilities between 2.0 and 6.0 kcal/mol (k_{rc} similar to k_{cl}) a mixed exchange process is predicted. The comparison of the simulated $\Delta G_{HX\ sim}$ and the nominal ΔG value at these conditions is represented in Fig. 4 *B*. Both ΔG values are coincident in the region of higher stability, 10.0 to 6.0 kcal/mol, where exchange occurs via the EX2 mechanism. Below this limit, $\Delta G_{HX\ sim}$ deviates and is larger than the corresponding nominal ΔG_{nom} value. Thus, when exchange rate data are analyzed by assuming that the EX2 mechanism holds, but exchange really occurs via a mixed mechanism or EX1 conditions, ΔG_{HX} will be overestimated. The effect of this incorrect assumption has been pointed out previously and accounts for the observation of ''superprotected'' amide groups (13,37–39). In our case, amide groups whose ΔG_{HX} is below 6.0 kcal/mol, do not exchange by a pure EX2 mechanism. Below 2.0 kcal/mol, the slope is less steep suggesting that the contribution of the exchange EX1 process is dominant.

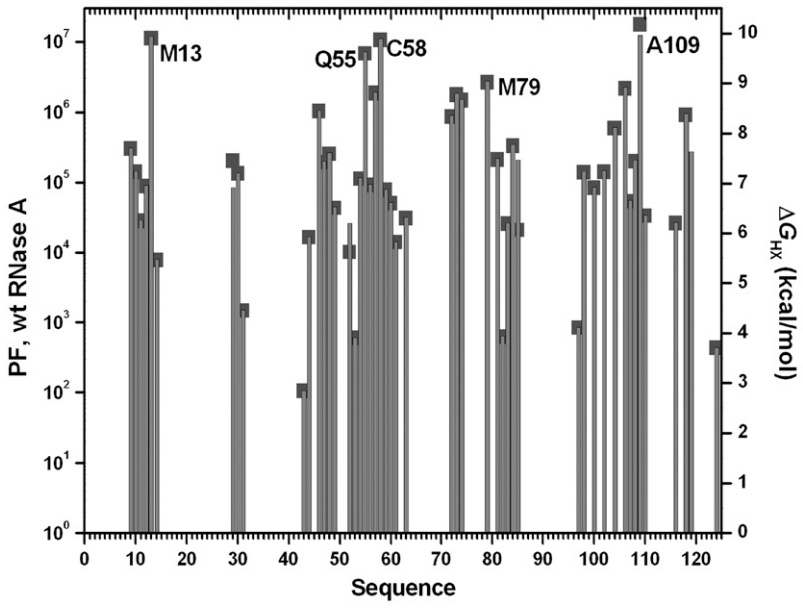

FIGURE 3 Conformational free energy of RNase A measured by hydrogen exchange. Protection factors (left *y* axis) and ΔG_{HX} (right *y* axis) for RNase A amide groups in D_2O at pH* 5.4 and 35°C. Gray squares are drawn to facilitate visualization of the maximum.

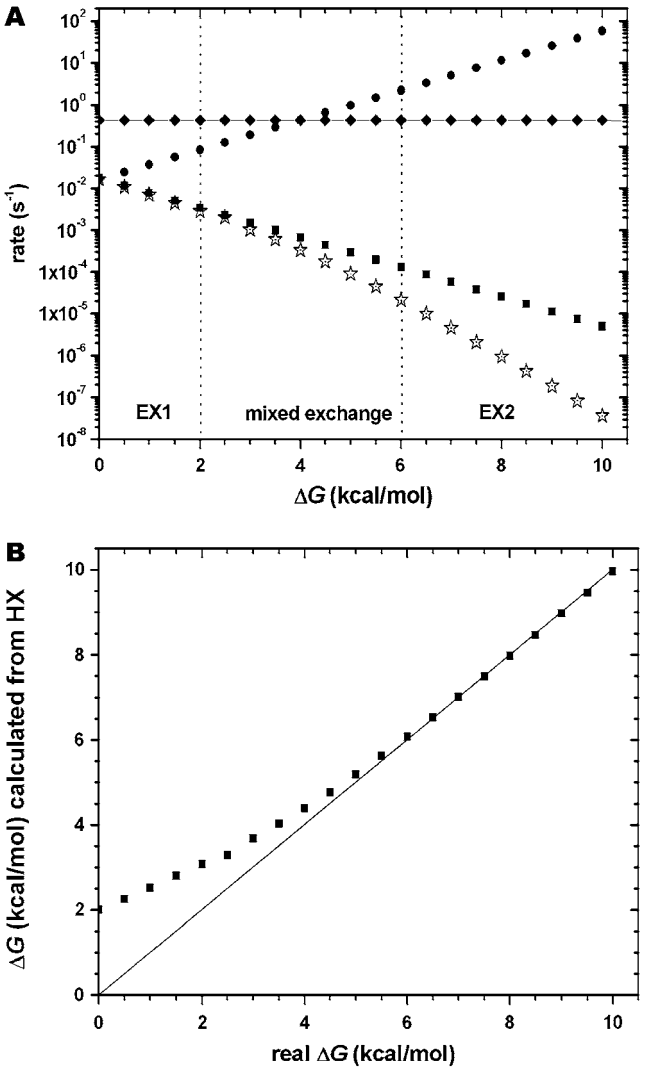

FIGURE 4 (*A*) Prediction of the H/D exchange mechanism of RNase A at 35°C and pH* 5.4 as a function of protein stability. The dependence of the individual rate constants is shown for k_{cl} (●), k_{op} (■), k_{rc} (♦), and $k_{ex\ sim}$ (☆). Three regions corresponding to pure EX1, EX2, or mixed exchange regime are shown according to the ratio between k_{cl} and k_{rc}. (*B*) Comparison of the calculated $\Delta G_{HX\ sim}$ from k_{ex}/k_{rc} values with the nominal $\Delta G_{HX\ nom}$ values of RNase A at 35°C and pH* 5.4.

For native wild-type RNase A, the exchange rates for the most protected protons are on the order of 10^{-7} to 10^{-8} s^{-1}, which corresponds to stabilities of 9.9 kcal/mol. Most of the observable amide protons have sufficient protection to exchange via the EX2 mechanism (compare Figs. 3 and 4 *A*), but there some, i.e., 43, 97, and 124, that are predicted to exchange by a mixed EX1 + EX2 mechanism.

H/D exchange measurements of ^{15}N-RNase A I106A and V108G variants

The H/D exchange experiments on the I106A mutant were done under the same conditions as wild-type RNase A. In these conditions the variant is stable enough to maintain the 3D structure and to produce high quality NMR spectra. The results of the protection factors at 35°C for I106A are represented in Fig. 5. Overall, the observable protection factors are lower in I106A than in wt RNase A, which indicates that the destabilizing effect of the mutations is propagated throughout the protein structure. Large differences between the exchange rates for wt RNase relative to the I106A variant are observed in the most stable regions, mainly in α-helices I (residues 9 and 13) and III (residues 55–58), and in β-strands IV (Met^{79}) and V (Ala^{109}). The number of protected NHs is similar in both proteins; the only amide protons that lose observable protection in I106A are Lys^{104} and the C-terminal Val^{124}.

The H/D exchange of V108G at 10°C is summarized in Fig. 6. As was reported previously, this mutant is very unstable at 35°C (4,17), the 3D structure is not maintained and as a consequence the NMR study could not be carried out in the same conditions as for the other mutants. H/D exchange measurements at 10°C ensure that this variant is stable and correctly folded as shown by chemical shift analysis (Fig. 2, see above). At this temperature, the exchange process could be followed at 52 individual HN protons, most of which belong to secondary structural elements. We have observed protection in the helical regions, especially in helix I (residues 6–14), helix II (residues 26–34), and the C-terminus of helix III (residues 56–61). The highest protection values are located in the Ala^{56}-Cys^{58} region (Fig. 6 *A*). Importantly, protection was also found in the region surrounding the mutated site.

The differences in the protection factors between wt RNase A and the variants are illustrated in Fig. 7. It is notable that loss of protection shows little correlation with the proximity to the mutated site.

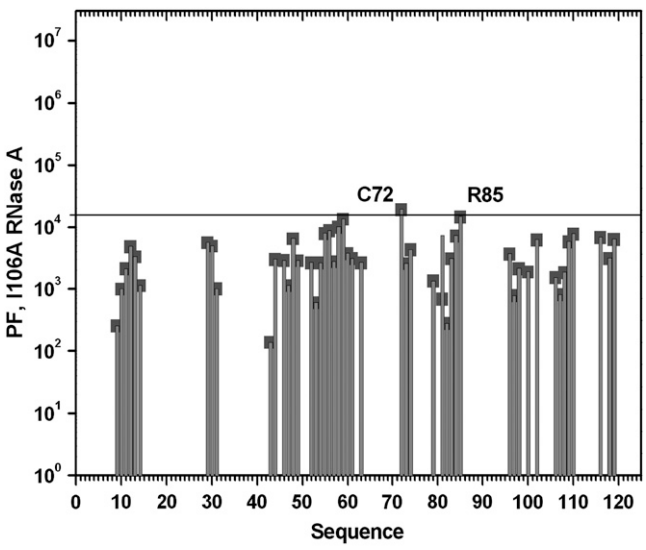

FIGURE 5 Protection factors for amide groups in D_2O at pH* 5.4 and 35°C of I106A RNase A variant measured by hydrogen exchange. Gray squares are drawn to facilitate visualization of the maximum.

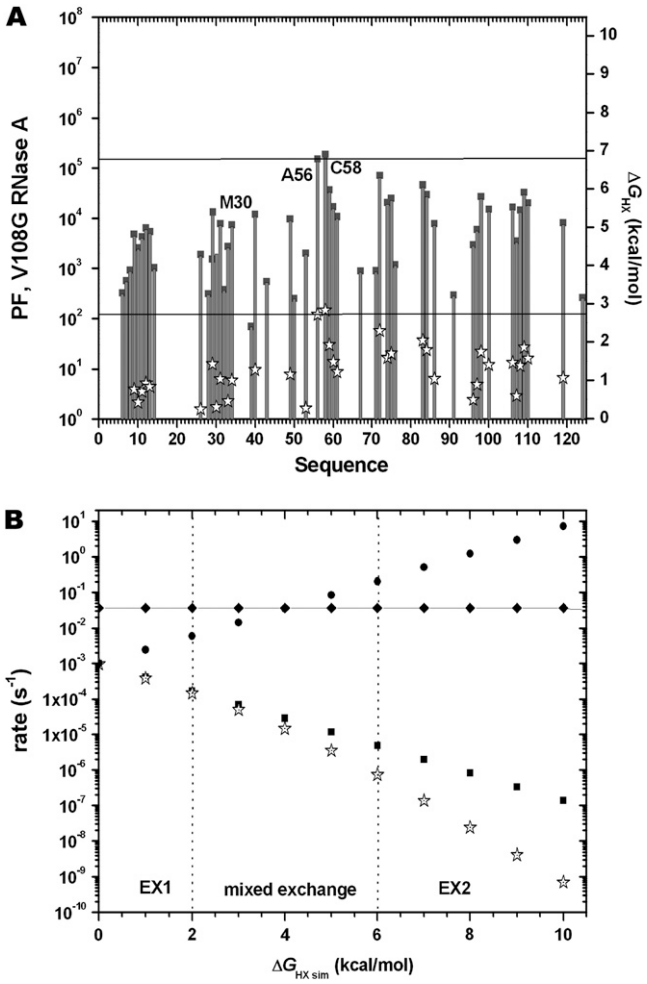

FIGURE 6 (*A*) Conformational free energy of V108G RNase A variant measured by hydrogen exchange. Protection factors (left *y* axis) and ΔG_{HX} (right *y* axis) for amide groups in D_2O at pH* 5.4 and 10°C. Stars represent the value of ΔG_{HX} minus 4 kcal/mol, which is the overall stability difference between 10°C and 35°C. Gray squares are drawn to facilitate visualization of the maximum. (*B*) Prediction of the H/D exchange mechanism of RNase A at 10°C and pH* 5.4 as a function of protein stability. The dependence of the individual rate constants is shown for k_{cl} (●), k_{op} (■), k_{rc} (♦), and $k_{ex\ sim}$ (☆).

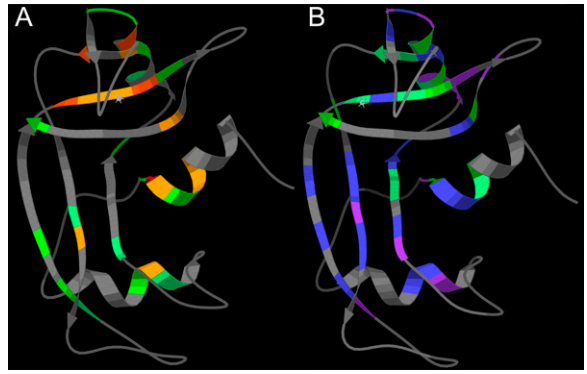

FIGURE 7 Ribbon diagram of RNase A variant V108G (*A*, *left panel*) and I106A (*B*, *right panel*), colored to indicate protection factors as log ΔPF decreases relative to wt RNase A: <1, violet; 1–2, blue; 2–3, sea blue; 3–4, green; 4–5, yellow; 5–6, orange; and >6, red. Gray indicates residues whose exchange could not be followed in the wt RNase A and/or the variant. The mutated residues are marked by stars. The log ΔPF for V108G has been adjusted to account for the temperature difference.

DISCUSSION

Effect of I106A and V108G mutations on the structure of RNase A

It has been shown that differences in the global stability of related proteins can be rationalized on the basis of global or local structural changes (40). In particular, when the wild-type protein and a mutant variant show large $\Delta\Delta G_{wt\text{-}mut}$ values, one can expect important structural rearrangements leading to the loss of additional native stabilizing interactions, and even to the formation of non-native pathological conformations (41). Our results show that other situations are possible. Residues belonging to the RNase A core are important for protein stability as was shown previously (28,42–44). Specifically, mutations in positions 106 and 108 destabilize the protein (4,17) but the results show that they have not altered the global fold. In this context, the similarity of the NMR data of the RNase A I106A and V108G variants with respect to the wild-type is especially relevant. It is well known that NMR chemical shifts are very sensitive to small structural perturbations (45). Thus, the lack of differences is solid evidence for the preservation of the native structure in these mutants under the specific experimental conditions. Interestingly, the effect of the mutations on the structure is localized to their immediate neighborhood, whereas their effect on the stability, as discussed below, is propagated throughout the whole molecule.

H/D exchange behavior and conformational stability of recombinant wild-type RNase A

Simulation and experimental data agree with previous results showing that hydrogen exchange data of wild-type RNase A at pH 5.4 and 35°C occurs in the EX2 regime. Therefore, protons exchanging via global unfolding may be used as indicators of global stability, and it has been found that, after correction for proline isomerization, these values should be close to ΔG_U obtained by calorimetric or chemical denaturation as it has been shown for a large number of proteins (46). Additionally, the H/D exchange method also allows the detection of the small-amplitude localized unfolding events.

When we compared the data obtained in this work with those published with nonrecombinant RNase A, we saw that the number and type of residues for which the exchange could be monitored are not exactly the same. Differences can be attributed to the different type of NMR spectra, homo- or heteronuclear, used in these studies. The exchange rates of

certain protected protons could not be measured in the ^{1}H-^{1}H homonuclear or ^{1}H-^{15}N heteronuclear spectra due to different signals being overlapped or obscured by the residual water signal. However, the exchange profile and the energy values at a residue level resemble those reported previously in similar conditions (at pH 5.5 and 34°C) (33). Regions with high ΔG_{HX} values defining exchange processes through global unfolding and through local unfolding are coincidental.

Simulation of RNase H/D exchange as a function of stability offers an approach to corroborate previous assumptions. The exchange data of RNase A was compared by Neira et al. (15) with that of RNase S to determine residues exchanging through the global or local fluctuations. In that study, an EX2 mechanism was probed for RNase A and assumed for RNase S on the basis of structure similarity and exchange data. At pH 6.0 and 35°C, RNase S is 3.8 kcal/mol less stable than RNase A as determined by thermal denaturation experiments (15). Simulations in these conditions (data not shown) agree with the reported experimental exchange rates and thus confirm the EX2 mechanism.

RNase I106A variant exchanges through a mixed EX2-EX1 mechanism: simulations and NMR data

Previous calorimetric data show that this mutant is 4.9 kcal/mol less stable than wild-type RNase A (4–7,17). According to exchange simulations, mixed exchange is predicted because under these conditions (around 5.0 kcal/mol), k_{cl} is similar to k_{rc}. H/D exchange studies carried out with destabilized mutants of barnase have also been shown to deviate from the EX2 behavior (14). In those cases, the contribution of the EX1 process could not be established unequivocally but the extent of deviation did seem to be related with the overall stability of the protein.

The exchange rates of the most protected NH groups in the I106A variant lie in the 10^{-5}–10^{-4} s^{-1} range. Because exchange occurs through a mixed EX1 + EX2 mechanism, one can not convert the exchange-rate information into ΔG_{HX} values. If one analyzes the I106A exchange data assuming that the EX2 mechanism was valid, a value for ΔG_{HX} of 6.0 ± 0.3 kcal/mol is obtained. Compared with RNase A in the same conditions (9.9 ± 0.5 kcal/mol), the difference (3.9 kcal/mol) is substantially smaller than the one reported on the basis of differential scanning calorimetry measurements, $\Delta\Delta G_{wt\text{-}I106A} = 4.9$ kcal/mol. This result is consistent with our prediction that applying the EX2 mechanism to calculate ΔG_{HX} when exchange really proceeds via EX1 or EX1 + EX2 leads to overestimates of ΔG_{HX} (Fig. 4 *B*).

This fact should be taken into account in ΔG_{HX} determinations especially when studying protein mutants with compromised stability. The consequence is that the energy gap separating local and the global unfolding is smaller and residues that exchange by non global unfolding in RNase A, exchange by a global process in the less stable I106A variant. As the stability of the protein is decreased, nearly all protected residues exchange concomitantly by global unfolding. This means that substitution of Ile by Ala in position 106 weakens the hydrophobic interactions that stabilize the protein core in the central β-sheet of RNase A without affecting the globular fold. This weakening affects the system globally, but particularly the most stable regions of RNase A. In fact, the per residue stability and loss of protection on mutation are correlated strongly ($R = 0.92$ and 0.88 for I106A and V108G, respectively). A similar dependence was observed for RNase A destabilized by GdmCl and interpreted using a model in which residues unfold locally regionally or globally (33). As the 3D structure is maintained, the loss of stability can be envisaged as a weakening of most of the molecular interactions, starting from the mutated regions and expanding throughout the protein. This is consistent with other results that point to this region to be the structural core of the RNase A, as well as a key initiator of its folding (1). Moreover, these results are in agreement with previous equilibrium studies showing that the main hydrophobic core of RNase A is tightly packed. Large changes in the number of methyl/ene groups have nonadditive positive stability interaction energies that are consistent with exquisitely tight core packing and rearrangements of the van der Waals' interactions in the protein interior, even after drastic deleterious substitutions (6).

Conformational stability of RNase V108G variant derived from H/D exchange

The analysis and the results of the V108G variant are completely different. The corresponding results can not be compared directly with those of wt RNase A or I106A as the temperature was not the same due to the low stability of the mutant. At 10°C, the V108G variant has a global conformational stability similar to that of I106A at 35°C. However, as the temperature is lower, k_{rc} and k_{op} are smaller and the exchange processes via the EX2 mechanism (Fig. 6 *B*) permitting the stability of the native state to be calculated on the basis of the exchange data. The highest stability values, ~6.8 kcal/mol, are located at the Ala^{56}-Cys^{58} region. Importantly, protection was also found in the region corresponding to the mutation V108G. RNase A V108G variant loses six interactions between Val^{108} and residues in the N-terminal α-helical region. If we compare the exchange profiles of the wt protein (Fig. 3) and this mutant (Fig. 6) we can see that whereas in the wt RNase A, helix I (3–13) and β-strand V (96–111) contribute some of the most protected NH groups, in V108G both regions show less protection than other parts of the protein. The magnitude of this great loss of stability is similar in both helix I and β-strand V. It is interesting to note that the loss of these interactions compromise the stability but not the integrity of the 3D structure.

To make a comparison with the wt protein and the I106A variant, the per residue ΔG_{HX} values of V108A at 35°C were

estimated. On the basis of the previously determined ΔH (95 kcal/mol) (47), T_m, and ΔC_p (2.2 kcal/mol) (48) and applying the Gibbs-Helmholtz equation, it was found that a correction factor of ~4 kcal/mol should be subtracted from the stability values measured at 10°C to estimate the stability at 35°C. These values are represented in Fig. 6 by stars. In this estimation, the global ΔG_{HX} drops to 2.8 kcal/mol; this is 7.1 kcal/mol less than wt RNase A. This difference falls short of the $\Delta\Delta G_{wt\text{-}V108G}$ determined by differential scanning calorimetry (9.3 kcal/mol). This discrepancy could arise from the fact that the unfolded state of RNase V108G variant is rarely populated and refolds completely under HX conditions (5°C), whereas it is the majority form present during thermal unfolding and seems to refold incompletely. The ratio between calorimetric and van 't Hoff enthalpies (R) of V108G is 0.5, which has been interpreted as proof of a deviation from the two-state unfolding model that is likely caused by self-association between molecules in the denaturation process (17). It is possible that the low stability of this variant favors self-association and that the unfolded state at high temperature is different than those of wt and I106A proteins whose calorimetry data are consistent with two-state denaturation.

Kinetic simulation as a tool to interpret hydrogen exchange results

Simulation of the kinetics of the hydrogen exchange process was used to identify the boundaries, in terms of stability, where exchange is governed by the EX1, mixed, or EX2 mechanisms. The findings suggest strongly that a single point mutation can be sufficient to switch the overall exchange mechanism. This result emphasizes the importance of these residues to the stability of RNase A.

One interesting result of this exercise is that the region of stability where mixed exchange occurs is rather large. This is due to the fact that k_{cl} must be much smaller than k_{rc} for exchange to be purely EX1 and k_{cl} must be much larger ("$\gg$" corresponds to a factor of $\approx$50) than k_{rc} for exchange to be purely EX2.

Although the approach described allows one to predict globally the boundaries between EX1, mixed, and EX2 exchange, one important caveat is that on the level of individual residues, k_{op} and k_{cl} can vary substantially. To cite one extreme case, Cys^{24} and Gly^{25} in ovomucoid third domain are both in the core of highly protected amide groups whose ΔG_{HX} values (of 7.4 and 7.5 kcal/mol, respectively) are very similar to each other and to the overall conformational stability measured by denaturant-induced unfolding, yet their k_{op} and k_{cl} values differ by more than a factor of 10 (49). For amide protons exchanging via local or regional unfolding events, k_{op} and k_{cl} will vary even more, as the residue-level stability of these groups is lower. The key implication is that within the same protein molecule the exchange regime can vary from EXI for weakly protected amide groups to EXII for strongly protected amide groups.

SUPPLEMENTARY MATERIAL

To view all of the supplemental files associated with this article, visit www.biophysj.org.

We thank Dr. J. L. Neira (Universidad Miguel Hernández, Elche, Spain) for insightful discussions.

This work was supported by the Spanish Ministerio de Educación y Ciencia (BFU2005-01855/BMC,BFU2006-15543-CO2-02).

REFERENCES

1. Neira, J. L., and M. Rico. 1997. Folding studies on ribonuclease A, a model protein. *Fold. Des.* 2:R1–R11.
2. Raines, R. T. 1998. Ribonuclease A. *Chem. Rev.* 98:1045–1066.
3. Chiti, F., and C. M. Dobson. 2006. Protein misfolding, functional amyloid, and human disease. *Annu. Rev. Biochem.* 75:333–366.
4. Torrent, J., J. P. Connelly, M. G. Coll, M. Ribó, R. Lange, and M. Vilanova. 1999. Pressure versus heat-induced unfolding of ribonuclease A: the case of hydrophobic interactions within a chain-folding initiation site. *Biochemistry.* 38:15952–15961.
5. Torrent, J., P. Rubens, M. Ribó, K. Heremans, and M. Vilanova. 2001. Pressure versus temperature unfolding of ribonuclease A: an FTIR spectroscopic characterization of 10 variants at the carboxy-terminal site. *Protein Sci.* 10:725–734.
6. Font, J., A. Benito, J. Torrent, R. Lange, M. Ribó, and M. Vilanova. 2006. Pressure- and temperature-induced unfolding studies: thermodynamics of core hydrophobicity and packing of ribonuclease A. *Biol. Chem.* 387:285–296.
7. Font, J., A. Benito, R. Lange, M. Ribó, and M. Vilanova. 2006. The contribution of the residues from the main hydrophobic core of ribonuclease A to its pressure-folding transition state. *Protein Sci.* 15: 1000–1009.
8. Huyghues-Despointes, B. M., C. N. Pace, S. W. Englander, and J. M. Scholtz. 2001. Measuring the conformational stability of a protein by hydrogen exchange. *Methods Mol. Biol.* 168:69–92.
9. Krishna, M. M., L. Hoang, Y. Lin, and S. W. Englander. 2004. Hydrogen exchange methods to study protein folding. *Methods.* 34:51–64.
10. Bai, Y. 2006. Protein folding pathways studied by pulsed- and native-state hydrogen exchange. *Chem. Rev.* 106:1757–1768.
11. Hvidt, A., and S. O. Nielsen. 1966. Hydrogen exchange in proteins. *Adv. Protein Chem.* 21:287–386.
12. Arrington, C. B., and A. D. Robertson. 1997. Microsecond protein folding kinetics from native-state hydrogen exchange. *Biochemistry.* 36:8686–8691.
13. Ferraro, D. M., N. D. Lazo, and A. D. Robertson. 2004. EX1 hydrogen exchange and protein folding. *Biochemistry.* 43:587–594.
14. Perrett, S., J. Clarke, A. M. Hounslow, and A. R. Fersht. 1995. Relationship between equilibrium amide proton exchange behavior and the folding pathway of barnase. *Biochemistry.* 34:9288–9298.
15. Neira, J. L., P. Sevilla, M. Menéndez, M. Bruix, and M. Rico. 1999. Hydrogen exchange in ribonuclease A and ribonuclease S: evidence for residual structure in the unfolded state under native conditions. *J. Mol. Biol.* 285:627–643.
16. Chakshusmathi, G., G. S. Ratnaparkhi, P. K. Madhu, and R. Varadarajan. 1999. Native-state hydrogen-exchange studies of a fragment complex can provide structural information about the isolated fragments. *Proc. Natl. Acad. Sci. USA.* 96:7899–7904.
17. Coll, M. G., I. I. Protasevich, J. Torrent, M. Ribó, V. M. Lobachov, A. A. Makarov, and M. Vilanova. 1999. Valine 108, a chain-folding initiation site belonging residue, crucial for the ribonuclease A stability. *Biochem. Biophys. Res. Commun.* 265:356–360.
18. Ribó, M., A. Benito, A. Canals, M. V. Nogués, C. M. Cuchillo, and M. Vilanova. 2001. Purification of engineered human pancreatic ribonuclease. *Methods Enzymol.* 341:221–234.

19. Kraulis, P. J. 1989. ANSIG: a program for the assignment of protein 1H 2D NMR spectra by interactive computer graphics. *J. Magn. Reson.* 24:627–633.

20. Rico, M., M. Bruix, J. Santoro, C. González, J. L. Neira, J. L. Nieto, and J. Herranz. 1989. Sequential 1H-NMR assignment and solution structure of bovine pancreatic ribonuclease A. *Eur. J. Biochem.* 183:623–638.

21. Rico, M., J. Santoro, C. González, M. Bruix, J. L. Neira, and J. L. Nieto. 1993. Refined solution structure of bovine pancreatic ribonuclease-A H-1-NMR methods. Side-chain dynamics. *Appl. Magn. Reson.* 4:385–415.

22. Bax, A., and D. G. Davis. 1985. MLEV-17-based two-dimensional homonuclear magnetization transfer spectroscopy. *J. Magn. Reson.* 65:355–360.

23. Kumar, A., R. R. Ernst, and K. Wüthrich. 1980. A two-dimensional nuclear Overhauser enhancement (2D NOE) experiment for the elucidation of complete proton-proton cross-relaxation networks in biological macromolecules. *Biochem. Biophys. Res. Commun.* 95:1–6.

24. Driscoll, P. C., G. M. Clore, D. Marion, P. T. Wingfield, and A. M. Gronenborn. 1990. Complete resonance assignment for the polypeptide backbone of interleukin 1 beta using three-dimensional heteronuclear NMR spectroscopy. *Biochemistry.* 29:3542–3556.

25. Bodenhausen, G., and D. J. Ruben. 1980. Natural abundance nitrogen-15 NMR by enhanced heteronuclear spectroscopy. *J. Chem. Phys. Lett.* 69:185–189.

26. Bai, Y., J. S. Milne, L. Mayne, and S. W. Englander. 1993. Primary structure effects on peptide group hydrogen exchange. *Proteins.* 17:75–86.

27. Molday, R. S., S. W. Englander, and R. G. Kallen. 1972. Primary structure effects on peptide group hydrogen exchange. *Biochemistry.* 11:150–158.

28. Font, J., J. Torrent, M. Ribó, D. V. Laurents, C. Balny, M. Vilanova, and R. Lange. 2006. Pressure-jump-induced kinetics reveals a hydration dependent folding/unfolding mechanism of ribonuclease A. *Biophys. J.* 91:2264–2274.

29. Kiefhaber, T., and F. X. Schmid. 1992. Kinetic coupling between protein folding and prolyl isomerization. II. Folding of ribonuclease A and ribonuclease T1. *J. Mol. Biol.* 224:231–240.

30. Barshop, B. A., R. F. Wrenn, and C. Frieden. 1983. Analysis of numerical methods for computer simulation of kinetic processes: development of KINSIM—a flexible, portable system. *Anal. Biochem.* 130:134–145.

31. Santoro, J., C. González, M. Bruix, J. L. Neira, J. L. Nieto, J. Herranz, and M. Rico. 1993. High-resolution three-dimensional structure of ribonuclease A in solution by nuclear magnetic resonance spectroscopy. *J. Mol. Biol.* 229:722–734.

32. Rico, M., J. Santoro, C. González, M. Bruix, J. L. Neira, J. L. Nieto, and J. Herranz. 1991. 3D structure of bovine pancreatic ribonuclease A in aqueous solution: an approach to tertiary structure determination from a small basis of 1H NMR NOE correlations. *J. Biomol. NMR.* 1:283–298.

33. Mayo, S. L., and R. L. Baldwin. 1993. Guanidinium chloride induction of partial unfolding in amide proton exchange in RNase A. *Science.* 262:873–876.

34. Wang, A., A. D. Robertson, and D. W. Bolen. 1995. Effects of a naturally occurring compatible osmolyte on the internal dynamics of ribonuclease A. *Biochemistry.* 34:15096–15104.

35. Qian, H., S. L. Mayo, and A. Morton. 1994. Protein hydrogen exchange in denaturant: quantitative analysis by a two-process model. *Biochemistry.* 33:8167–8171.

36. Loh, S. N., C. A. Rohl, T. Kiefhaber, and R. L. Baldwin. 1996. A general two process model describes the hydrogen exchange behavior of RNase A in unfolding conditions. *Proc. Natl. Acad. Sci. USA.* 93: 1982–1987.

37. Clarke, J., and A. R. Fersht. 1996. An evaluation of the use of hydrogen exchange at equilibrium to probe intermediates on the protein folding pathway. *Fold. Des.* 1:243–254.

38. Swint-Kruse, L., and A. D. Robertson. 1996. Temperature and pH dependences of hydrogen exchange and global stability for ovomucoid third domain. *Biochemistry.* 35:171–180.

39. Qu, Y., and D. W. Bolen. 2003. Hydrogen exchange kinetics of RNase A and the urea: TMAO paradigm. *Biochemistry.* 42:5837–5849.

40. Huyghues-Despointes, B. M., U. Langhorst, J. Steyaert, C. N. Pace, and J. M. Scholtz. 1999. Hydrogen-exchange stabilities of RNase T1 and variants with buried and solvent-exposed Ala → Gly mutations in the helix. *Biochemistry.* 38:16481–16490.

41. Jiang, X., J. N. Buxbaum, and J. W. Kelly. 2001. The V122I cardiomyopathy variant of transthyretin increases the velocity of rate-limiting tetramer dissociation, resulting in accelerated amyloidosis. *Proc. Natl. Acad. Sci. USA.* 98:14943–14948.

42. Chatani, E., K. Nonomura, R. Hayashi, C. Balny, and R. Lange. 2002. Comparison of heat- and pressure-induced unfolding of ribonuclease a: the critical role of Phe46 which appears to belong to a new hydrophobic chain folding initiation site. *Biochemistry.* 41:4567–4574.

43. Iwaoka, M., W. J. Wedemeyer, and H. A. Scheraga. 1999. Conformational unfolding studies of three-disulfide mutants of bovine pancreatic ribonuclease A and the coupling of proline isomerization to disulfide redox reactions. *Biochemistry.* 38:2805–2815.

44. Schultz, D. A., and R. L. Baldwin. 1992. Cis proline mutants of ribonuclease A. I. Thermal stability. *Protein Sci.* 1:910–916.

45. Anderson, D. E., J. Lu, L. McIntosh, and F. W. Dahlquist. 1993. The Folding, Stability and Dynamics of T4 Lysozyme: A Perspective Using Nuclear Magnetic Resonance. CRC Press, Boca Raton, FL.

46. Huyghues-Despointes, B. M., J. M. Scholtz, and C. N. Pace. 1999. Protein conformational stabilities can be determined from hydrogen exchange rates. *Nat. Struct. Biol.* 6:910–912.

47. Freire, E., and R. L. Biltonen. 1978. Thermodynamics of transfer ribonucleic acids: the effect of sodium on the thermal unfolding of yeast tRNAPhe. *Biopolymers.* 17:1257–1272.

48. Pace, C. N., and D. V. Laurents. 1989. A new method for determining the heat capacity change for protein folding. *Biochemistry.* 28:2520–2525.

49. Arrington, C. B., L. M. Teesch, and A. D. Robertson. 1999. Defining protein ensembles with native-state NH exchange: kinetics of interconversion and cooperative units from combined NMR and MS analysis. *J. Mol. Biol.* 285:1265–1275.

50. Koradi, R., M. Billeter, and K. Wuthrich. 1996. MOLMOL: a program for display and analysis of macromolecular structures. *J. Mol. Graph.* 14:51–55, 29–32.